

Search-based Kinodynamic Motion Planning for Omnidirectional Quadruped Robots*

Pei Wang, Sihan Zhang, Qingteng Zhao, Jun Wu, Qiuguo Zhu¹

Abstract—Autonomous navigation has played an increasingly significant role in quadruped robots system. However, existing works on path planning used traditional search-based or sample-based methods which did not consider the kinodynamic characteristics of quadruped robots. And paths generated by these methods contain kinodynamically infeasible parts, which are difficult to track. In the present work, we introduced a complete navigation system considering the omnidirectional abilities of quadruped robots. First, we use kinodynamic path finding method to obtain smooth, dynamically feasible, time-optimal initial paths and added collision cost as a soft constraint to ensure safety. Then the trajectory is refined by timed elastic band (TEB) method based on the omnidirectional model of quadruped robot. The superior performance of our work is demonstrated through simulated comparisons and by using our quadruped robot Jueying Mini in our experiments.

I. INTRODUCTION

Legged robots have better mobility and versality than wheeled or tracked vehicles in complex environment such as rough terrains. However, research on legged robots has been limited because of the difficulty and complexity of building and controlling technology. In competitions, such as the DARPA Robotics Challenge and the ARGOS Challenge, some of the best research groups gather together to solve real-world problems, which has resulted in many high-performance robots. Comparatively, multi-legged robots have better speed, flexibility, and stability than bipedal robots in locomotion, including ETH's ANYmal [1], IIT's HyQ [2] and HyQ2Max [3], MIT's Cheetah [4], Cheetah II [5] and Cheetah III [6], Boston Dynamics' Spot and SpotMini, a direct successor to Big Dog [7]. These robots focused more on precise control and strong locomotive capabilities, and rarely on autonomous navigation capabilities. To date, SpotMini has shown autonomous navigation capabilities, whereas Big Dog used a variation of the A* algorithm for path planning and a spline algorithm for path smoothing [8]. ANYmal featured the A* algorithm for pose graph planning and the RRT* algorithm for traversability planning [9]. However, none of these methods takes into account legged robot kinematic characteristics. Other planning methods include search-based methods, such as Anytime repairing A* [10], Lifelong planning A* [11], and D* [12], or sampled-based methods, such as RRT [13] and Informed RRT* [14]. However, these

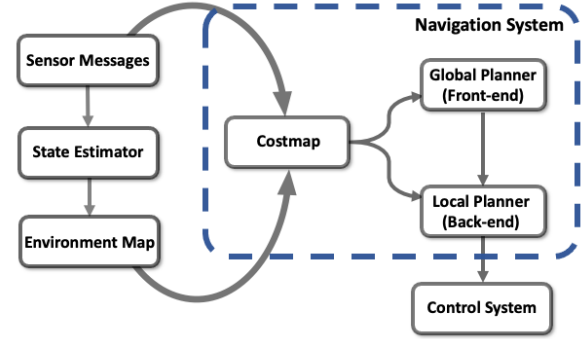


Figure 1. The structure of navigation system

methods do not consider kinodynamic characteristics, which may increase the burden of back-end optimization. Kinodynamic path finding, which originated from the hybrid-state A* algorithm that was first proposed for autonomous vehicles [15], identifies a smooth, safe, and kinodynamically feasible path. Its performance was related to the robot model type. So far, kinodynamic method has been verified in unmanned aerial [16] and wheeled vehicles but has not yet been proven in quadruped robots. Thus, our work introduced a planning algorithm and navigation system for the quadruped robot platform Jueying Mini, with consideration of its unique motion ability. The main contribution of this paper can be concluded as

1) According to omnidirectional locomotion of quadruped robot, a kinodynamic path finding method is used in the front-end, instead of geometric graph searching, for smooth, collision-free, dynamically feasible, and time-optimal control trajectories. These trajectories are easily tracked and can reduce the burden of back-end for trajectory optimization. Hard and soft constraints with costmap are introduced to ensure safe front-end searching.

2) We use the timed elastic band (TEB) method under omnidirectional locomotion model for back-end trajectory optimization and add constraints according to actual physical parameters and different locomotive abilities (in the forward-backward and lateral directions of our quadruped robot).

Section II of this paper describes the navigation system's structure and formulates the navigation problem. Section III introduces the Kinodynamic A* algorithm and describes hard and soft constraints applied to the motion uncertainty optimization problem. In Section IV, we combine TEB and omnidirectional methods for quadruped robots to refine the front-end path planning. Section V describes the experiments that we used to verify the robot's performance and presents results. In Section VI, we summarize our work.

*This work was supported by the Science and Technology Project of Zhejiang Province (2019C02003).

Qiuguo Zhu is with the State Key Laboratory of Industrial Control Technology and Institute of Cyber-Systems and Control, Zhejiang University, Zhejiang, 310027, China (corresponding author; email: qgzhu@zju.edu.cn).

Pei Wang, Sihan Zhang, Qingteng Zhao, Jun Wu are with the State Key Laboratory of Industrial Control Technology and Institute of Cyber-Systems and Control, Zhejiang University, Zhejiang, 310027, China

II. PROBLEM FORMULATION

A. System Overview

The planning system framework is shown in Fig. 1. The framework has three important components: Costmap, Global planner, and Local planner. Costmap takes sensor input of the real environment and inflates costs on a 2D occupancy grid map. Global planner generates an initial trajectory, containing kinodynamic information, from the current position to goal position. Local planner, using TEB, obtains the robot's real-time location from the state estimator, provides a controller that connects path to robot, generates a trajectory, and sends motion commands to robot control system.

B. Problem Formulation and Assumptions

Jueying Mini [17] is a quadruped robot that has the ability to move in a wide variety of complex environments. The control system guarantees the stability, and provides omnidirectional mobility to the robot. Since motion planning is in two dimensional regions, and roll and pitch can be ignored while their values remain small, only forward-backward, lateral, and yaw motions. This allows translation and rotation to be defined independently of one other and simplifies the planning problem.

III. KINODYNAMIC A* PATH FINDING METHOD

A. Motion Primitives Generation

Based on the assumption in Section II.B, each axis component of trajectory can be described independently. Let $x(t) \in \chi \subset \mathbb{R}^{2n}$ be a system state, consisting of position $p(t)$ and its $n-1$ derivatives (velocity, acceleration, etc.). Thus,

$$x(t) := [p(t)^T, \dot{p}(t)^T, \dots, p^{(n-1)}(t)^T]^T$$

$$p(t) := [p_x(t), p_y(t)], p_d(t) = \sum_{k=0}^K a_k \frac{t^k}{k!}, d \in \{x, y\} \quad (1)$$

The velocity is denoted by $v(t) := \dot{p}(t)$, and also acceleration is denoted by $a(t) := \ddot{p}(t)$, and the control input $u(t) = p^{(n)}(t) \in U := [-u_{max}, u_{max}]^2 \subset \mathbb{R}^2$. The state space model can be described as

$$\dot{x} = Ax + Bu, \quad (2)$$

$$A = \begin{bmatrix} 0 & I_2 & 0 & \cdots & 0 \\ 0 & 0 & I_2 & \cdots & 0 \\ & \vdots & & \ddots & \vdots \\ 0 & 0 & 0 & \cdots & I_2 \\ 0 & 0 & 0 & \cdots & 0 \end{bmatrix}, B = \begin{bmatrix} 0 \\ 0 \\ \vdots \\ 0 \\ I_2 \end{bmatrix}$$

The solution for the equation is expressed as

$$x(t) = e^{At} x(0) + \int_0^t e^{A(t-\tau)} + Bu(\tau) d\tau \quad (3)$$

To generate trajectories that consider more than the shortest geometric distance considered by the traditional A* algorithm, i.e., that are also smooth, collision-free,

dynamically feasible, and optimal (in time and control), the qualities of the trajectory can be expressed as

$$J(\phi) = \int_0^T u(t)^2 dt = \int_0^T p^{(n)}(t)^2 dt \quad (4)$$

where ϕ denotes the trajectory. By taking time into consideration, the cost function is refined to

$$J(T) = J(\phi) + \rho T = \int_0^T u(t)^2 dt + \rho T \quad (5)$$

where ρ is the parameter which determines the relative importance of the duration versus its smoothness.

The problem defined by (5) is a linear quadratic minimum-time problem [18]. To convert the optimization problem into a graph searching problem [16], we used lattice discretization $U_M := \{u_1, u_2, \dots, u_M\}$, and each control input $u_m \in \mathbb{R}^2$ is a vector in the x - y plane, which is applied for a short duration τ . A discretization step d_μ was introduced to get $\mu = u_{max}/d_\mu$ samples along each axis $[0, u_{max}]$. Then, the discretized set of $(2\mu+1)^2$ primitives was $\{-u_{max}, -\delta(\mu-1)u_{max}, \dots, 0, \dots, \delta(\mu-1)u_{max}, u_{max}\}$, $\delta = 1/\mu$. Since τ is short, we treat the control input as a constant vector u_m . Using the initial state $x_0 := [p_0^T, v_0^T, \dots]^T$, another form of $p_d(t)$ is written as

$$p_d(t) = u_m \frac{t^n}{n!} + \dots + v_0 t + p_0 \quad (6)$$

Both duration and control input are known and fixed, we calculate the actual cost of a motion primitive as $(\|u_m\|^2 + \rho)\tau$. And the actual cost g from the start state to the current state is accumulated as $\sum (\|u_m\|^2 + \rho)\tau$.

B. Heuristic Function

A suitable heuristic function reduces unnecessary expansion and results in faster searching. The distance between the current state and the goal state is heuristic for the traditional A* algorithm. Since the evaluation of g has changed, and the complexity of the Kinodynamic A* algorithm is higher than that of A*, it is essential to design an admissible and tight heuristic function to speed up node expansion. By minimizing $J(T)$ from the current state to the goal state, using the Pontryagins minimum principle [19] where $n = 2$, we get

$$p_d^*(t) = \frac{1}{6} \alpha_d t^3 + \frac{1}{2} \beta_d t^2 + v_{dc} + p_{dc}$$

$$\begin{bmatrix} \alpha_d \\ \beta_d \end{bmatrix} = \frac{1}{T^3} \begin{bmatrix} -12 & 6T \\ 6T & -2T^2 \end{bmatrix} \begin{bmatrix} p_{dg} - p_{dc} - v_{dc}T \\ v_{dg} - v_{dc} \end{bmatrix}$$

$$J^*(T) = \sum_{d \in \{x,y\}} \left(\frac{1}{3} \alpha_d^2 T^3 + \alpha_d \beta_d T^2 + \beta_d^2 T \right) \quad (7)$$

where p_{dc} , v_{dc} , p_{dg} , v_{dg} are the position and velocity of the current state and position and velocity of the goal state, respectively. The heuristic function $h = J^*(T)$ is only related to T . To minimize $J^*(T)$ for the optimal T , we need to obtain its extremum by making $\partial J^*(T) / \partial T = 0$. Denoting the root as T_h , we get $h = J^*(T_h)$ and $f = g + h = g + J^*(T_h)$.

C. Collision and Dynamic Feasible Check

We aim to find a collision-free and dynamic feasible trajectory from the start state to the goal state. Hence, it is necessary to verify collision and dynamic constraints during the search process.

The environment is described with a two-dimensional occupancy grid map. The costmap, in which each grid has a value describing the probability of collision, can be generated based on the occupancy grid map. A set of positions that the system can traverse along the trajectory can be sampled using the cost map. We define a lethal cost, related to the size of robot, that represent the collision boundary as a hard constraint. For the duration τ , we need to ensure that the cost of each grid, corresponding to positions $p(t_i)$ for all $i \in \{0, \dots, I\}$, $t_i \in [0, \tau]$, is no more than the lethal cost. The selection of I should guarantee that the maximum distance between two adjacent sampling points does not exceed costmap resolution R by setting the condition $\tau v_{max} / I \geq R$.

The way to determine that the primitive satisfied the dynamic constraints, is to find the maximum and minimum derivatives, such as velocity and acceleration, during τ . Because the derivatives are polynomial function of time, we can easily obtain their extrema and check if they are within the constraints.

D. Soft Constraint for Safety

Although we obtain a collision-free trajectory with hard constraints, considering motion uncertainty, we prefer a trajectory that is as far away from obstacles as possible. Artificial Potential Field (APF) [20] is an efficient and commonly used method to maintain a path away from obstacles. However, it ignores dynamic constraints during re-optimization, and the resulting trajectory is often easily trapped in undesired local minima. Liu [21] models motion uncertainty as a soft constraint through the collision cost with an expression form of APF, but it requires a prior trajectory, from which the resulting trajectory is constrained to be within a tunnel.

A collision cost J_c was added to (5) as a soft constraint during the searching process:

$$J = J(\phi) + \rho T + \rho_c J_c \quad (8)$$

where ρ_c is the weight coefficient about collision description and J_c is defined according to trajectory

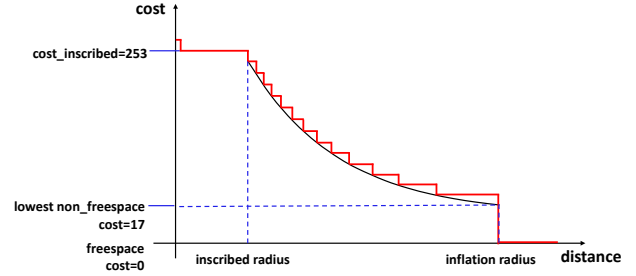


Figure 2. Trend of cost value in the costmap.

$$J_c(\phi) = \int_{\phi} F(s) ds, s \in \mathbb{R}^2 \quad (9)$$

$F(s)$ is the cost in position, and it depends on the costmap value

$$F(s) = \begin{cases} 0, & d(s) \geq d_{inflation} \\ f(d(s)), & d_{inflation} > d(s) \geq d_{lethal} \end{cases} \quad (10)$$

where $d(s)$ is the distance between the position s and the nearest obstacle. The inflation radius $d_{inflation}$ can be affected by the environment and safety demands. Points outside the inflation radius are considered safe. The inscribed radius of the robot is d_{lethal} . For the points between d_{lethal} and $d_{inflation}$, the cost is defined by

$$f(d) = f_{max} e^{-\lambda_c (d - d_{lethal})} \quad (11)$$

where λ_c determines the decreasing rate of cost value while $d \in [d_{lethal}, d_{inflation}]$. Different from previous works [20][21], gradient of cost function is not continuous and the range and trend can be adjusted by the inflation radius and the parameter λ_c , which may result in sharp decreases at the boundary (Fig. 2).

In practice, we can calculate the accumulated cost of each primitive by sampling. Similar to the process of collision checks, we obtain a set of I_c dense points along primitives during time τ . I_c is determined by

$$I_c = \frac{v_{max} \tau}{R} \quad (12)$$

where R is the resolution of the costmap. Start and end points of a primitive are included, so that the time step $dt := \tau / (I_c - 1)$. And the integral can be discretized as

$$\int_{\phi} F(s) ds \approx \sum_{i=0}^{I_c-1} F(p_{i_c}) \|v_{i_c}\| dt \quad (13)$$

where p_{i_c} and v_{i_c} are the position and velocity at time $i_c \cdot dt$. Therefore, the evaluation function that produces a trajectory away from obstacles, ensuring safety of robots, is

$$f = g + h + \rho_c c_{collision} \quad (14)$$

and the influence of collision cost can be adjusted by adjusting the weight ρ_c .

IV. TIMED ELASTIC BAND TRAJECTORY OPTIMIZATION

The trajectory generated by Kinodynamic A* provides not only a collision-free path but also time information, with which we can refine the prior path for a smoother and safer trajectory using the TEB approach. TEB is based on elastic band approach, defined by B : a sequence of n robot poses $s_i = [x_i, y_i, \beta_i]^T \in \mathbb{R}^2 \times S^1$ and $n-1$ time intervals ΔT_i . And x_i, y_i is the position, while β_i is the orientation of the robot in global frame. These can be written as

$$Q = \{s_i\}_{i=0 \dots n}, n \in \mathbb{N}, \tau = \{\Delta T_i\}_{i=0 \dots n-1}$$

$$B := (Q, \tau) \quad (15)$$

A total objective function

$$f(B) = \sum_k \gamma_k f_k(B)$$

$$B^* = \underset{B}{\operatorname{argmin}} f(B) \quad (16)$$

where B^* represents the optimized TEB. And component objective functions $f_k(B)$ contain constraints about the minimum time, attraction of global path, repulsion of obstacles with respect to trajectory, and dynamic limits, such as velocity and acceleration [22]. Because of the robot's omnidirectional properties, we obtain expressions for dynamic constraints that differ from those in [23]:

$$\Delta s_i = \begin{pmatrix} \Delta x_i \\ \Delta y_i \end{pmatrix} = \begin{pmatrix} x_{i+1} - x_i \\ y_{i+1} - y_i \end{pmatrix}$$

$$\Delta \theta_i = \theta_{i+1} - \theta_i \quad (17)$$

where Δs_i is the distance between consecutive positions x_i, x_{i+1} , $\Delta \theta_i$ is the angular change between the two position vectors. We convert Δs_i in time ΔT_i from the world coordinate system to the robot coordinate system using

$$dx_i = \Delta x_i \cos \theta_i + \Delta y_i \sin \theta_i$$

$$dy_i = -\Delta x_i \sin \theta_i + \Delta y_i \cos \theta_i \quad (18)$$

after which, linear and angular velocity and acceleration can then be obtained as

$$v_{ix} = \frac{dx_i}{\Delta T_i}, v_{iy} = \frac{dy_i}{\Delta T_i}, \rho_c = 5$$

$$a_{ix} = \frac{v_{(i+1)x} - v_{ix}}{(\Delta T_i + \Delta T_{i+1})/2}, a_{iy} = \frac{v_{(i+1)y} - v_{iy}}{(\Delta T_i + \Delta T_{i+1})/2}$$

$$\omega_i = \frac{\Delta \theta_i}{\Delta T_i}$$

$$\alpha_i = \frac{\omega_{i+1} - \omega_i}{(\Delta T_i + \Delta T_{i+1})/2} \quad (19)$$

V. EXPERIMENTAL RESULTS

A. Platform Details

Jueying Mini has four legs with 12 actuators, each leg has 3 degrees of freedom and each joint has an expanded range of motion. (Fig. 3) The kinodynamic constraints in navigation of Jueying Mini are shown in Table I. Jueying Mini is equipped with Velodyne VLP-16 LiDAR and IMU for sensing and state estimation. All software modules, including state estimation, mapping, and planning, run on a four-core 2.80 GHz processor with a 256 GB and 8 GB RAM.



Figure 3. The Jueying Mini quadruped robot.

TABLE I. KINODYNAMIC CONSTRAINTS IN EXPERIMENTS

Name	Value	Unit
max_vel_x	0.75	m/s
max_vel_y	0.20	
max_vel_theta	0.70	rad/s
acc_lim_x	1.00	m/s ²
acc_lim_y	0.17	
acc_lim_theta	0.52	rad/s ²

B. Simulations

1) *Search-Based Planning Performance*: To evaluate the Kinodynamic A* algorithm, we compare its performance with that of the traditional A* path planning algorithm. The results cannot be obtained directly, since the path generated by traditional A* does not contain any kinodynamic information. We use the data from actual trajectory. With the only difference between experiments lies in front-end, we can verify the performance between Kinodynamic A* and traditional A*.

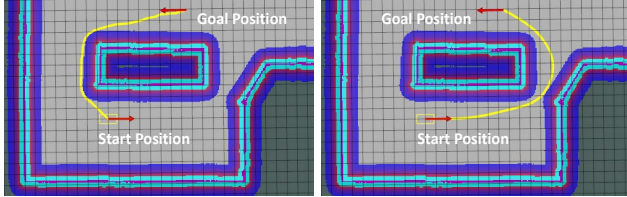
The experiment was performed on a simulated irregular polygon map approximately 30 m \times 30 m, with data recorded during navigation to evaluate the performance of two methods. As shown in Table II, the start and goal positions of four groups were randomly selected. For Kinodynamic A*, the effort of trajectory and the total running time for each experiment was better than those of the traditional A*. Kinodynamic A* resulted in a smoother and more easily tracked prior path, while the path of traditional A* had many

dynamically infeasible parts, which required more energy and time for the local planner to optimize and adjust. Therefore, we demonstrate that Kinodynamic A* algorithm can finally lead to a smooth and fast trajectory to execute.

TABLE II. COMPARISON OF PATH PLANNING ALGORITHMS.

	Total Running Time (s)		Effort J	
	<i>Kinodynamic A*</i>	<i>Traditional A*</i>	<i>Kinodynamic A*</i>	<i>Traditional A*</i>
1	27.362	31.794	4.7630	5.5047
2	16.298	25.395	5.1730	6.8421
3	25.338	31.000	5.1201	5.8651
4	25.975	25.594	4.1946	7.4720

Another advantage of Kinodynamic A* is that it takes kinodynamic characteristics into consideration. As shown in Fig.4, the global planner using A* contains no motion information, it ignores the initial state, especially in re-planning. This may result in trajectories that are unsuitable. However, Kinodynamic A* considers the robot's initial state and avoids the unnecessary cost of turning around.



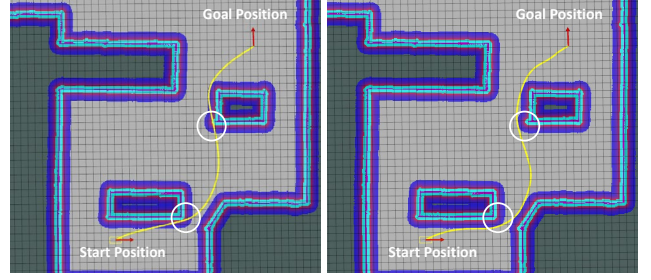
(a) Traditional A* (b) Kinodynamic A*

Figure 4. Dynamic feasibility performance. The yellow rectangle represents the outline, the yellow line represents the path, and the red arrow represents the position vector of the robot.

2) *Collision Cost Performance*: We verified the contribution of soft collision constraints. Fig. 5(a) shows results of the method without soft constraints, in which the robot may hit the obstacle inside the circle region. Fig. 5(b) shows the results of the method with collision costs, in which the robot avoids the obstacles by walking a safer path.

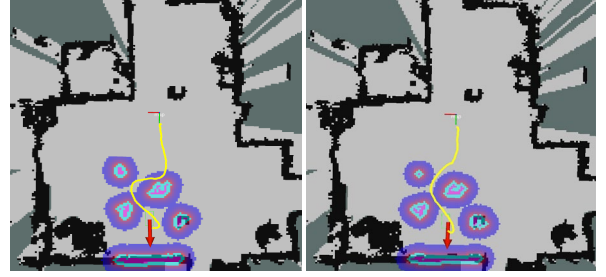
C. Experiments

1) *Search-Based Planning Performance*: We conducted the experiment in an incompletely known environment with



(a) Kinodynamic A*, $\rho_c=0$ (b) Kinodynamic A*, $\rho_c=5$

Figure 5. Performance after adding a collision cost. The collision cost can be achieved by adjusting ρ_c . The yellow rectangle represents the outline, the yellow line represents the path, and the red arrow represents the position vector of the robot.



(a) Traditional A* (b) Kinodynamic A*

Figure 6. The actual trajectories of the robot. The yellow line represents the actual trajectory of the robot and the red arrow represents the position vector of the robot.

unexpected obstacles, unknown in the initial costmap. Fig. 6 shows the actual trajectories of the robot. The Kinodynamic A* algorithm provided an easily tracked prior trajectory which led to a better final trajectory, while the trajectory produced by the traditional A* algorithm had many dynamically infeasible parts that made tracking difficult for the local planner.

2) *Omnidirectional Method Performance*: We compared omnidirectional model performance with that of the non-omnidirectional model performance for TEB in an indoor environment as shown in Fig. 7. The overall running time of each experiment was compared. Because of the difference in forward and lateral locomotion abilities, we set a greater weight for the forward direction. As shown in Table III and Fig. 7, the omnidirectional method was flexible and fast. Because the omnidirectional motion characteristics of the

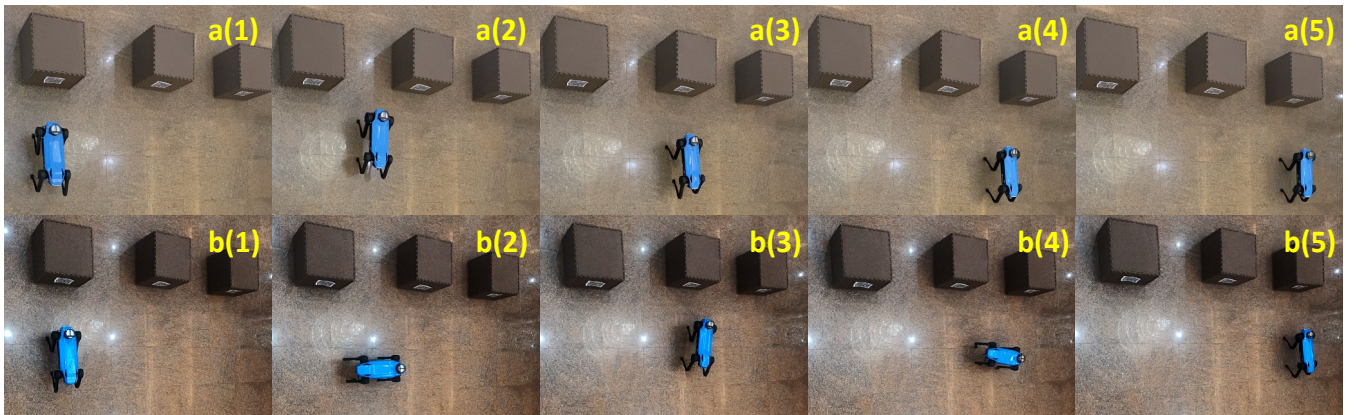


Figure 7. Three parallel points are set up to simulate a situation where the robot is performing actual tasks. The robot needs to face toward the object and stay for 2s. The upper pictures show the performance of the omnidirectional method, and the lower one shows the performance of the non-omnidirectional method.



Figure 8. Dynamic obstacle avoidance performance.

quadruped robot were considered, our method enabled robot to transfer flexibly between the parallel points by side shifting.

TABLE III. COMPARISON OF OMNIDIRECTIONAL AND NONOMNIDIRECTIONAL METHODS

	Time(s)	
	<i>Omnidirectional method</i>	<i>Non-omnidirectional method</i>
To first via points	11	11
To second via points	10	20
To third via points	11	23
Total time	32	54

3) *Dynamic Obstacle Avoidance*: We test the robot in a dynamic and completely unknown environment as shown in Fig.8. Perception range limits prevented some obstacles from being considered in the initial global plan, which was a challenge to planning, requiring continuous and rapid re-planning to avoid sudden dangers. As shown in Fig. 8, our method can generate feasible trajectories and allow the robot to flexibly react. Additional details can be seen in our accompanying video.

VI. CONCLUSION

In this paper, we described the design of a complete autonomous navigation system for quadruped robots that takes into account their ability for flexible, powerful, and stable omnidirectional locomotion. We used a framework with a global planner and a local planner, to find a path from start to goal and calculate velocity commands for robot to execute. The global planner uses Kinodynamic A* to find a smooth, safe, kinodynamically feasible, and minimum-time prior path, which contains hard and soft constraints to guarantee the clearance and dynamic feasibility. The initial path is refined by local planner using TEB method with an omnidirectional model. Finally, we verified the effectiveness and feasibility of our method through experiments and proved that our quadruped robot can perform more flexible movements and react rapidly to changes in complex environments.

REFERENCES

- [1] Hutter M, Marco C, Lauber A, et al. "Anymal-toward legged robots for harsh environments." *Advanced Robotics* 31.17 (2017): 918-931.
- [2] Semini C, Tsagarakis N G, Guglielmino E, et al. "Design of HyQ—a hydraulically and electrically actuated quadruped robot." *Proceedings of the Institution of Mechanical Engineers, Part I: Journal of Systems and Control Engineering* 225.6 (2011): 831-849.
- [3] Semini C, Barasuol V, Goldsmith J, et al. "Design of the hydraulically actuated, torque-controlled quadruped robot HyQ2Max." *IEEE/ASME Transactions on Mechatronics* 22.2 (2016): 635-646.
- [4] Seok S, Wang A, Chuah M Y, et al. "Design principles for energy-efficient legged locomotion and implementation on the MIT cheetah robot." *IEEE/ASME transactions on mechatronics* 20.3 (2014): 1117-1129.H.
- [5] Park H W, Wensing P M, and Kim S. "High-speed bounding with the MIT Cheetah 2: Control design and experiments." *The International Journal of Robotics Research* 36.2 (2017): 167-192.
- [6] Di C, Wensing P M, Katz B, et al. "Dynamic locomotion in the mit cheetah 3 through convex model-predictive control." *2018 IEEE/RSJ International Conference on Intelligent Robots and Systems (IROS)*. IEEE, 2018.
- [7] Raibert M, Blankespoor K, Nelson G, et al. "Bigdog, the rough-terrain quadruped robot." *IFAC Proceedings Volumes* 41.2 (2008): 10822-10825.
- [8] Wooden D, Malchano M, Blankespoor K, et al. "Autonomous navigation for BigDog." *2010 IEEE International Conference on Robotics and Automation*. IEEE, 2010.
- [9] Bellicoso C D, Bjelonic M, Wellhausen L, et al. "Advances in real-world applications for legged robots." *Journal of Field Robotics* 35.8 (2018): 1311-1326.
- [10] Likhachev M, Ferguson D, Gordon G, et al. "Anytime search in dynamic graphs." *Artificial Intelligence* 172.14 (2008): 1613-1643.
- [11] Koenig S, Likhachev M, and Furey D. "Lifelong planning A*." *Artificial Intelligence* 155.1-2 (2004): 93-146.
- [12] Stentz, Anthony. "Optimal and efficient path planning for partially known environments." *Intelligent unmanned ground vehicles*. Springer, Boston, MA, 1997. 203-220.
- [13] LaValle, Steven M., and James J. Kuffner Jr. "Randomized kinodynamic planning." *The international journal of robotics research* 20.5 (2001): 378-400.
- [14] Gammell, Jonathan D., Timothy D. Barfoot, et al. "Informed sampling for asymptotically optimal path planning." *IEEE Transactions on Robotics* 34.4 (2018): 966-984.
- [15] Dolgov D, Thrun S, Montemerlo M, et al. "Path planning for autonomous vehicles in unknown semi-structured environments." *The International Journal of Robotics Research* 29.5 (2010): 485-501.
- [16] Liu S, Atanasov N, Mohta K, et al. "Search-based motion planning for quadrotors using linear quadratic minimum time control." *2017 IEEE/RSJ international conference on intelligent robots and systems (IROS)*. IEEE, (2017):2872-2879.
- [17] <http://www.deeprobotics.cn/>
- [18] Verriest, E. I., and F. L. Lewis. "On the linear quadratic minimum-time problem." *IEEE transactions on automatic control* 36.7 (1991): 859-863.
- [19] Mueller M W, Hehn M, and D'Andrea R. "A computationally efficient motion primitive for quadcopter trajectory generation." *IEEE Transactions on Robotics* 31.6 (2015): 1294-1310.

- [20] Li G, Tamura Y, Yamashita A, et al. "Effective improved artificial potential field-based regression search method for autonomous mobile robot path planning." *International Journal of Mechatronics and Automation* 3.3 (2013): 141-170.
- [21] Liu S, Mohta K, Atanasov N, et al. "Towards search-based motion planning for micro aerial vehicles." *arXiv preprint arXiv:1810.03071* (2018).
- [22] Rösmann C, Feiten W, Wösch T, et al. "Efficient trajectory optimization using a sparse model." *2013 European Conference on Mobile Robots*. IEEE, 2013.
- [23] Rösmann C, Feiten W, Wösch T, et al. "Trajectory modification considering dynamic constraints of autonomous robots." *ROBOTIK 2012; 7th German Conference on Robotics*. VDE, 2012.